Chinese Journal of
POLYMER SCIENCE

RESEARCH ARTICLE

https://doi.org/10.1007/s10118-023-3056-6
Chinese J. Polym. Sci. **2024**, *42*, 437–445

Thermo- and pH-sensitive Polymer with Pendant Spacer-linked Imidazole Cycles

Natalya V. Zakharova[a*], Stanislav N. Zelinskiy[b], Mariya S. Strelova[b], Elena N. Danilovtseva[b], and Vadim V. Annenkov[b]

[a] *Institute of Macromolecular Compounds of the Russian Academy of Sciences, Saint Petersburg 199004, Russia*
[b] *Limnological Institute of Siberian Branch of the Russian Academy of Sciences, Irkutsk 664033, Russia*

Abstract By the reaction of poly(acryloyl chloride) with *N*-(3-aminopropyl)imidazole, poly(*N*-(3-(1*H*-imidazol-1-yl)propyl)acrylamide) was synthesized. The new polymer contains an imidazole ring removed from the main chain by a spacer of five bonds. The structure and purity, molecular weight, hydrodynamic and thermosensitive properties of the obtained sample were studied by ^{1}H- and ^{13}C-NMR, FTIR spectroscopy, acid-base titration, light scattering, turbidimetry and viscometry. The observed ability of the imidazole-containing polymer to form and destroy associates in water-salt solutions at pH 6.6–7.4 and temperatures of 29–48 °C indicates that these are promising candidates for designing complex biomedical systems. The new polymer is able to form complexes with oligo-DNA more actively than poly(1-vinylimidazole), which is of interest for gene delivery applications. The polymer cross-linked with epichlorohydrin gives micro-relief coatings on the plastic surface, and the modified surface is able to attach negatively charged objects. This thermo- and pH-sensitive polymer modification can be applied to create finely controlled surfaces for cell culturing.

Keywords Imidazole-containing polymer; Thermolability; pH-sensitivity; The modified surface; DNA immobilization

Citation: Zakharova, N. V.; Zelinskiy, S. N.; Strelova, M. S.; Danilovtseva, E. N.; Annenkov, V. V. Thermo- and pH-sensitive polymer with pendant spacer-linked imidazole cycles. *Chinese J. Polym. Sci.* **2024**, *42*, 437–445.

INTRODUCTION

In recent years, much attention has been paid to the development of "smart" polymers for drug delivery systems and other biomedical applications.[1–6] Thermo- and pH-sensitive polymers can respond to small changes in the environment and exhibit a reversible phase transition in aqueous solution.[7–9] There are many potential biomedical and pharmaceutical applications related to thermo- and pH-sensitive polymers, especially in drug delivery systems, including gene therapy.[10–14]

Polymeric amines are used in many applications, including industry, biocidal compounds, and components of pharmaceutical compositions.[15–19] Polymers containing amine groups and hydrophobic fragments exhibit dual thermo- and pH-sensitivity in an aqueous medium.[20–22] Biomedical and related applications require sensitivity in the neutral area, at pH 6–8. The pK_a of the conjugated acids of aliphatic amines exceeds 9.5, and these groups are significantly protonated in the neutral area, which prevents thermo-sensitivity in this pH region. N-substituted imidazoles show less basicity (pK_a of methylimidazole is 7–7.4).[23–26] Poly(1-vinylimidazole) (PVI) has been known for decades as a low-base water-soluble polymer.[27–30] This polymer is based on a commercially available monomer, and numerous copolymers and more complex structures have been prepared starting from 1-vinylimidazole. The high buffer capacity of PVI and its ability to coordinate with nucleic acids allow imidazole cycles to be considered as components of gene delivery agents.[31] pK_0 of abstraction of the last proton from the conjugated polyacid PVI is 6.0 in 0.1 mol/L NaCl, and protonation of PVI reduces its basicity due to the electrostatic effect.[32] Because of the low degree of protonation in the neutral pH region, PVI can give an H-bonded complex at the pyridine nitrogen atom, which is impossible for protonated amine groups.

1-(3-Aminoprolyl)imidazole (API) is another compound promising for the introduction of imidazole molecules into polymer structures. It contains a primary amine group that is active in the reaction with chloroanhydrides, activated esters, *etc*. The presence of a trimethylene fragment allows the construction of structures with an imidazole cycle distanced from the main polymer chain and other cycles. API was used to develop synthetic amphiphilic polypeptides.[33,34] The interaction of API with methacryloyl chloride resulted in the formation of an imidazole-containing monomer, which was copolymerized with *N*-isopropylacrylamide, giving a thermosensitive polymer.[35] API itself contains a hydrophobic fragment, and we can expect thermal sensitivity from a polymer containing only API-based units. The most similar to such a poly-

* Corresponding author, E-mail: Na_Zar@inbox.ru
Received August 9, 2023; Accepted September 24, 2023; Published online November 17, 2023

mer are API-terminated dendrimers.[36] These dendrimers show high pH sensitivity in the neutral region, but the thermal sensitivity of these compounds has not been studied. There is evidence that the distancing of the imidazole cycle from the main chain causes the cycles to behave independently.[36,37]

This work is aimed at the synthesis of poly(*N*-(3-(1*H*-imidazol-1-yl)propyl)acrylamide) (PIPAA) as a polymer each unit of which contains an imidazole cycle removed from the main chain with a five-bond spacer. PIPA was obtained by reacting poly(acryloyl chloride) with API in the same way as the synthesis of pH- and thermo-sensitive polymers based on amines.[7,38] This is the first API-based homopolymer, and the study of its acid-base and thermal properties is necessary to design more complex structures. The potential of the new polymer for the design of oligonucleotide carriers and functional surfaces is also discussed.

MATERIALS AND METHODS

Materials

Dimethylformamide (DMF), acryloyl chloride, triethylamine, 1-(3-aminopropyl)imidazole, AIBN, NaCl, HCl, NaOH, and other chemicals were of reagent grade (Merck, Fisher, or Acros Chemicals). Deuterium oxide (D_2O, 99.8 atom D%) was purchased from Sigma-Aldrich. NBD-N3 dye was synthesized according to.[39] PVI was synthesized by radical polymerization of VI in benzene at 60 °C in the presence of AIBN in an argon atmosphere.[40] DMF was dried with anhydrous $CuSO_4$ and 3-Å molecular sieves, followed by distillation. AIBN was recrystallized from ethanol. NaOH was purified from carbonate impurities by filtering its 50% solutions. Thermo Scientific SnakeSkin Dialysis Tubing (3.5K MWCO, 22 mm) was applied for the dialysis. Sartorius syringe membrane filters 0.45 μm (cellulose nitrate) were used for filtration. Deionized water (resistivity 18.2 MΩ·cm) was used from a purification system of Millipore Simplicity UV (USA). Fluorescein 3'-tagged DNA oligonucleotide GATCTCATCAGGGTACTCCTT was purchased from Evrogen JSC (Russia).

Synthesis of PIPAA

Poly(acryloyl chloride) (PACh) prepared from 16.22 mmol of acryloyl chloride by the reported method,[41] was dissolved in 17.79 g of DMFA dried over 3 Å zeolites. The solution was cooled in an ice bath and a mixture of triethylamine (1.90 g, 18.8 mmol), 1-(3-aminopropyl)imidazole (2.33 g, 18.6 mmol) and DMF (2 mL) was poured into it at one time while stirring on a magnetic stirrer (Scheme 1). The resulting turbid mixture was continued to stir under refrigeration for another 10 min and then left at room temperature for 24 h, after which it was diluted with 100 mL of distilled water, the pH of the solution was adjusted to ~7, and the solution was dialyzed (3.5 kDa) for 8 days relative to distilled water. After filtration through a 0.45 μm cellulose acetate filter, the solution was concentrated on a rotary evaporator and lyophilically dried. The polymer yield was 1.577 g.

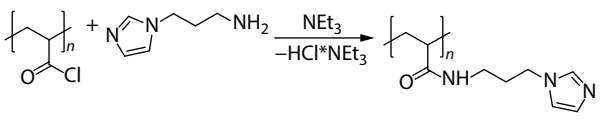

Scheme 1 Reaction scheme for the production of PIPAA.

^{1}H-NMR (400 MHz, D_2O, δ, ppm): 1.0–1.8 (C$\underline{H}_2$ main chain), 1.8–2.5 (C$\underline{H}$ main chain, CC$\underline{H}_2$C (prolyl)), 2.9–3.3 (NHC$\underline{H}_2$C), 3.5–3.7 (C$\underline{H}$ main chain), 3.9–4.2 (CC$\underline{H}_2$N), 4.8 (H_2O), 6.8–7.4 (NC$\underline{H}$C$\underline{H}$N ring), 7.7–8.2 (NC$\underline{H}$N ring). ^{13}C-NMR (100 MHz, D_2O, δ, ppm): 29–30 (C$\underline{H}_2$ main chain), 33–38 (NH$\underline{C}H_2\underline{C}H_2$), 41–43 (C$\underline{H}$ main chain), 43–46 ($CH_2\underline{C}H_2$N), 119–121 (N$\underline{C}$HCHN ring), 124–127 (NCH$\underline{C}$HN ring), 135–137 (N$\underline{C}$HN ring), 175–178 (C(O)N).

^{1}H-NMR and FTIR Spectroscopy

The chemical structure of the polymer prepared was identified using ^{1}H- and ^{13}C-NMR spectra. ^{1}H- and ^{13}C-NMR spectra were recorded on a DPX 400 Bruker instrument (Bruker Biospin Corporation, Billerica, MA, USA) in D_2O at 400.13 MHz for ^{1}H and 100.62 MHz for ^{13}C-NMR. IR spectra were recorded with an Infralum FT-801 spectrometer (SC Simex, Novosibirsk, Russia) using KBr pellets. To record FTIR spectrum of the hydrochloride of PIPAA, a solution of the polymer in methanol was saturated with gaseous HCl and the volatiles were distilled off under reduced pressure. To record FTIR spectrum of basic PIPAA, an aqueous solution of the polymer was adjusted to pH 10 with addition of KOH and freeze dried.

Molecular Weight Determination

Determination of molecular weight and hydrodynamic characteristics of imidazole-containing polymer (PIPAA)

The molecular weight of the PIPAA sample and the hydrodynamic radius $R_{h\text{-}D}$ of macromolecules were measured by static and dynamic light scattering in dilute solutions in buffer (Hanna Instruments, pH=7.01). Light scattering was studied on a Photocor Complex instrument (Photocor Instruments Inc., Russia); the light source was a Photocor-DL diode laser (power, 5–30 mW; wavelength, λ=659.1 nm). The calibration of the device, that is, the determination of the instrument coefficient, was carried out using toluene (R_V=1.38×10^{-5} cm^{-1}). The measurements were performed at scattering angles θ in the range 45°–135°.

The correlation function of the scattered light intensity was recorded using a PhotocorPC_2 correlator with 288 channels and processed using DynalS software (ver. 8.2.3, SoftScientific, Tirat Carmel, Israel). The experiments were carried out at a temperature of 21.0 °C.

The refractive index increments dn/dc were measured using a RA-620 (λ=589.3 nm) refractometer (KEM, Japan). The refractive index increment dn/dc=0.1791±0.0090 cm^3/g in buffer, pH=7.01 was measured.

Intrinsic viscosity [η] was measured in buffer, pH = 7.01 with Ostwald viscometer at 21 °C. (The viscosimetry experiments were carried out on the Ostwald-type Cannon-Manning capillary viscometer (Cannon Instrument Company Inc., State College, PA, USA).

Light Transmittance and Dynamic Light Scattering

Investigation of self-assembly of PIPAA in buffer solutions

The aqueous and buffer solutions of the PIPAA samples were investigated by the methods of static (SLS) and dynamic (DLS) light scattering and turbidimetry using the Photocor Complex described above, which is also equipped with the Photocor-PD detection device for measuring the transmitted light intensity. The solution temperature T was changed discretely with the step ranging from 0.5 °C to 5.0 °C. The temperature was regulated with the precision of 0.1 °C. The T values changed in the

range of 13 °C to 75 °C. The buffers with pH=7.01 (Hanna Instruments, USA), 6.20, 6.86, 7.20 and 7.35, 7.40 (Hepes, PBS) were applied. After a desired temperature was achieved, all experimental characteristics began to change over time and reached constant values over time τ_{eq}. At steady-state conditions, *i.e.*, when the solutions parameters do not depend on time, the intensity I of scattered light, optical transparence I^*, hydrodynamic radii R_h of the scattering species, and their contribution S_i to the integral scattering intensity were determined. S_i was estimated using the values of the areas under the corresponding R_h distribution peak. These measurements were carried out at a scattering angle range of between 45° and 135° to prove the diffusion nature of the modes. To maintain linearity of the instrument with respect to I, the amount of fixed light scattering was attenuated by filters and by reducing the laser power so that the measured value of it did not exceed 1.2 MHz.

Potentiometric Titration of PIPAA

PIPAA and PVI were dissolved in DI water, 0.1 mol/L NaCl was added after dissolution of polymers. Polymers were titrated with 0.1M HCl from alkaline region (pH 11.5 was obtained by adding 0.1 mol/L NaOH). The pH of all solutions was determined using a "Multitest" ionometer (JSC Semico, Novosibirsk, Russian Federation) with a combined pH electrode at 20±0.1 °C and polymer concentration was 7.5 mmol/L. Buffer capacity of the polymers was calculated from the potentiometry data according to the IUPAC recommendations as a derivative of the added HCl concentration versus pH (the number of moles of strong base required to change the pH by one unit when added to one liter of the solution).[42]

Synthesis and Electrophoresis of Oligonucleotide Complexes with PIPAA Polymer

The interaction between 21-mer DNA oligonucleotide GATCTCATCAGGGTACTCCTT-6-FAM and PIPAA was investigated by electrophoresis on agarose gel. Complexes were prepared by mixing solution of polymer (2 g/L) and oligonucleotide (10 μmol/L). The samples were incubated at room temperature for 30 min and placed in the wells of 1% agarose gel. Controls for free oligonucleotide was also loaded to the gel. The gel running buffer was 40 mmol/L Tris acetate (pH adjusted to pH 7.4) and 1 mmol/L ethylenediaminetetraacetic acid (EDTA). A glycerol gel loading buffer was applied (0.5% sodium dodecyl sulfate, 0.1 mol/L EDTA (pH=7.4), 50% glycerol for 10x reagent). The gel was run at 90 V and the fluorescein-tagged oligonucleotide was visualized on a UV transilluminator.

Coating the Bottom of A 24-Well Microbiological Plate with Plastic Film

Ethanol solution (0.2 mL) containing 0.1% PIPAA, 5% (by weight of polymer) epichlorohydrin, and 5% (by weight of polymer) 2-pentanol was placed in the well of the plate. The covered plate was dried 48 h at room temperature, 12 h at 40 °C and 2 h at 90 °C. The coating was visualized under the action of poly(acrylic acid) (PAA) and fluorescent dye NBD-N3.[43] 0.2% PAA solution (0.2 mL, M_v=285 kDa) was added to the well for 5 min. The PAA solution was removed, the well was washed with water, and 0.02 mL of 0.09% aqueous NBD-N3 solution was added for 5 min. Fluorescence images were obtained using a MOTIC AE-31T inverted microscope with an HBO 103 W/2 OSRAM mercury vapor lamp, excitation was at 470 nm.

RESULTS AND DISCUSSION

Polymer Synthesis

The reaction between PACh and 1-(3-aminopropyl)imidazole in the presence of triethylamine led to obtaining a light-yellow polymer powder soluble in water (pH<7), ethanol, methanol, but insoluble in dichloromethane, acetone, diethyl ether. The ^{1}H-NMR spectrum (Fig. 1) has signals at 6.8–8.2 ppm from imidazole ring protons and at 1–4.5 ppm from protons of the main chain and propyl moiety. The integral intensities of the peaks are in good agreement with the polymer structure. The small peak at 3.57 ppm can be attributed to a minor rotamer of the amide group. Such rotamers have been described for low molecular weight compounds,[44,45] and steric hindrances from the polymer chain can increase this phenomenon. The complete substitution of chlorine atoms by 1-(3-aminopropyl)imidazole was also confirmed by the absence of the signal at 184 ppm (the ^{13}C-NMR spectrum) from carbons of carboxyl groups formed by hydrolysis of the residual acid chloride groups (Fig. 1).

The FTIR spectrum of PIPAA contains bands from vibrations of imidazole ring: 3105 (n CH ring), 1512 (ring), 1232 (d CH ring, n C—H ring), 1107 (d CH ring), 1085 (d CH ring, n ring), 746 (g CH, g ring), 662 cm^{-1} (n N—C, d ring);[46] amide bonds: 1520–1560 (amide 2), 1630–1740 (amide 1, C=O); main chain 1440–1460 cm^{-1} (CH_2). The signal at 1170 cm^{-1} (Fig. 2) indicates the presence of protonated imidazole groups in PIPAA.[46]

The fraction of protonated units in PIPAA was determined by potentiometric titration with 0.1 mol/L HCl from the alkaline region. Part of the added NaOH is used to neutralize the hydrochloric acid in the polymer, and the inflection in the titration curve in the alkaline region corresponds to the neu-

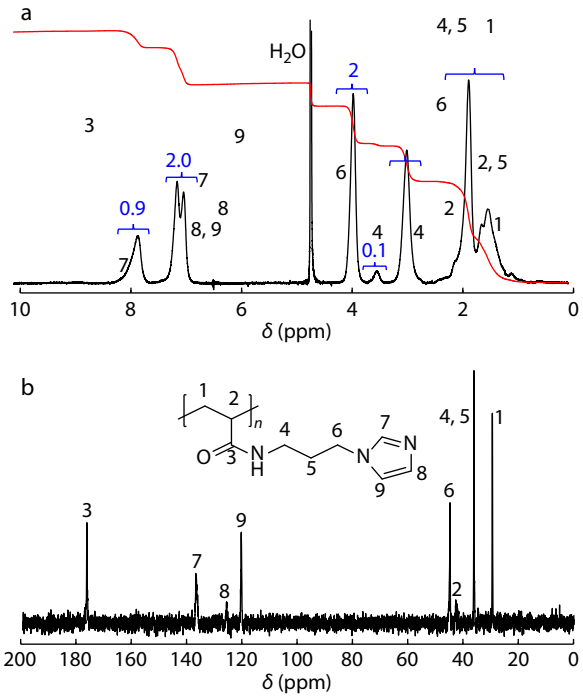

Fig. 1 (a) ^{1}H- and (b) ^{13}C-NMR spectra of PIPAA in D_2O. The relative integrated intensities of the peaks in the ^{1}H spectrum are represented by blue figures.

https://doi.org/10.1007/s10118-023-3056-6

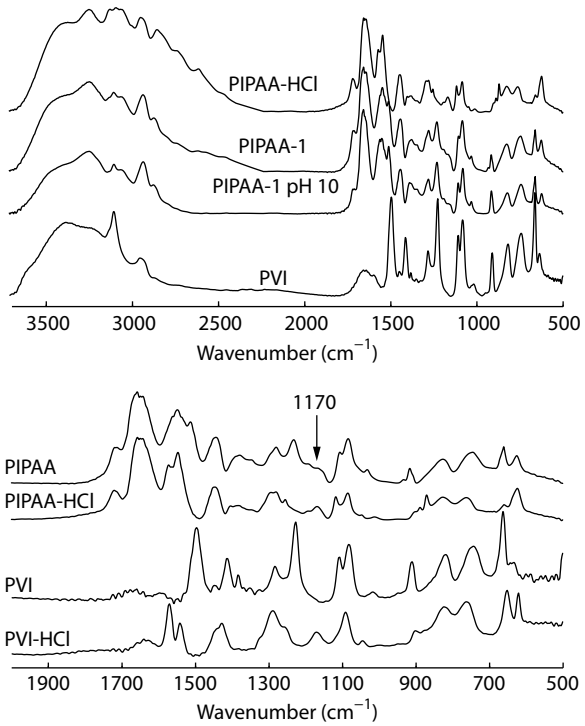

Fig. 2 FTIR spectra of the polymers in KBr pellets.

tralization of excess NaOH. The difference between the volume of added alkali and the inflection volume corresponds to the content of 28% protonated imidazole groups.

Polymer Solubility

PIPAA is soluble in water and acidic media; at pH>7 it precipitates (Table 1), in contrast to PVI, which is soluble in the entire studied pH range from 2.5 to 11.5. In an aqueous solution, in the absence of low-molecular-weight salts (NaCl, NaH_2PO_4), the PIPAA polymer is also soluble at pH>9.6, which may be due to the interaction of OH^- ions with imidazole cycles and the resulting electrostatic repulsion.[32] When the acid is added to an alkaline polymer solution, OH^- ions bind protons, thereby reducing the negative charge of the macromolecules. When neutrality is reached, the polymer chains collapse which is manifested by the polymer precipitation.

Thus, PIPAA is not soluble in water at pH above 7 but the presence of buffers allows to obtain solutions at pH 7.4. The buffers used contain a phosphate anion or (4-(2-hydroxyethyl)-1-piperazineethanesulfonic acid). In both cases we have compounds bearing groups active in the formation of hydrogen bonds: P—OH, ≡NH$^+$, C—OH. Imidazole units contain donor nitrogen atoms, and the bonding of these atoms with ions from the buffers increases the hydrophilicity and solubility of the polymer. It seems that sodium ions in phosphate buffer are preferable to potassium for PIPAA solubility, since pure sodium buffer significantly increases T_1. Sodium cations are more active in coordination with imidazole cycles[32] which may explain this effect. On the other hand, NaCl does not have the same effect, so the phosphate anion is also necessary to stabilize PIPAA macromolecules in aqueous solutions.

Acid-base Properties of PIPAA in Aqueous Solution

For PIPAA, the observed pK values are higher than those for PVI (Fig. 3). In PIPAA, the imidazole rings are located far from the main chain, their interaction with each other is weakened, and the "neighbor effect" observed in the case of polybases,[47] which reduces the basicity upon protonation of neighboring units, is generally less pronounced.

For PVI, pK changes monotonically as the degree of ionization of the conjugated acid decreases. In the case of PIPAA, the pK-α curve has three regions: two regions of a sharp decrease in pK upon decreasing α separated by a plateau, where a change in α has no effect on the pK value. Due to the presence of hydrophobic —$(CH_2)_3$— fragments in PIPAA, macromolecules tend to acquire a more compact conformation in the aqueous medium. When a neutral compacted macromolecule is protonated (on the plot, this corresponds to a de-

Table 1 Particle size and phase separation temperatures for PIPAA in water solutions.

Buffer	pH	c (g/L)	R_h (nm) at 21 °C	T_1 (°C)	T_2 (°C)	ΔT (°C)
Water	6.76	10.6	3.1 and 86.0 (S_s/S_f=9)	No separation up to 75 °C		
Water + one drop of 0.01 mol/L NaOH	7.10	10.6	Turbid dispersion			
"6.86"	6.86	10.4	3.3	34.5	36	1.5
		3.19	3.3	35.0	39	4
		0.983	3.1	35.5	43.0	7.5
		0.296	3.0	36.0	53	17.0
"Hanna"	7.01	2.90	3,1	29.0	31.0	2.0
		0.940	3.1	30.0	34.0	4.0
		0.300	3.1	38.0	48.0	10.0
"PBS"	7.40	3.13	3.3	46.0	48.0	2.0
"HEPES"	7.20	9.27		Transparent film-like sediment		
	7.2	2.00		* Turbid dispersion		
	7.28	1.00	–	* No separation up to 70 °C		
	7.35	1.00		Transparent film-like sediment		
	7.4	3.00		* Turbid dispersion		
		1.00		Turbid dispersion		
"HEPES" 0.1 mol/L	7.4	1.00		Turbid dispersion		

Buffers: "6.86" – KH_2PO_4 25 mmol/L, Na_2HPO_4 25 mmol/L; "Hanna" – KH_2PO_4 25 mmol/L, Na_2HPO_4 37 mmol/L; "PBS" – NaCl 137 mmol/L, KCl 2.7 mmol/L, Na_2HPO_4 10 mmol/L, KH_2PO_4 1.8 mmol/L; "HEPES" – 0.05 mol/L HEPES solution; * Polymer was dissolved in Water, after 3 h HEPES 0.1 mol/L was added, final HEPES 0.05 mol/L.

https://doi.org/10.1007/s10118-023-3056-6

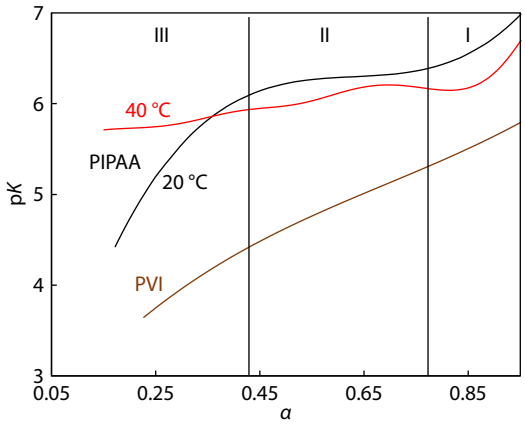

Fig. 3 p*K* of conjugated acid PIPAA and PVI as functions of the ionization degree.

crease in α from the region α=1), the basicity decreases with an increase in the positive charge of macromolecules (region I). After reaching a certain degree of ionization, the electrostatic repulsion forces begin to prevail over the hydrophobic interactions that favor compactization, and the macromolecule unfolds, this compensates the decrease in p*K* (region II). The next drop in p*K* at 20 °C (region III) is due to the protonation of the unfolded macromolecule. This phenomenon is analogous to the well-known flat part on the p*K*-α PMAA curves.[48] Region III is absent at 20 °C due to increased hydrophobic interactions at elevated temperatures and greater stabilization of the compact conformation.

Viscometry data confirm protonation of PIPAA at pH 6.8, the concentration dependence of the intrinsic viscosity (Fig. 4) shows a typical polyelectrolyte effect.

Molecular Weight Characteristics of PIPAA

Unfortunately, it was difficult to choose an appropriate solvent for this system. True solvents, in which only macromolecules exist, are salt solutions-buffers, where the salts are various potassium phosphates and hydrogen phosphates. One of these buffers is the Hanna buffer (USA). In other solvents, the molecular weight cannot be measured due to association in water (and polyelectrolyte effect in aqueous solutions) or the complete insolubility of the polymer in these solvents (such are chloroform, DMF, saline and 0.1 N KBr solution).

For the studied solutions in the concentration range c, a unimodal distribution was obtained by dynamic light scattering. The values of the hydrodynamic radius $R_{h\text{-}D}(c)$ were independent of c. Therefore, the concentration average value $R_{h\text{-}D}(c)$ was taken as the hydrodynamic radius $R_{h\text{-}D}$ for the macromolecules of the investigated polymer. The values of $R_{h\text{-}D}$ determined in buffer, pH=7.01, is 3.6±0.4 nm (Fig. 5). There was no asymmetry of light scattering; therefore, the M_w of the polymer was assessed by the Debye method.[49,50] The obtained value of the second virial coefficient (A_2 = (−9.6±1.0)×10^{-5} cm^3·mol/g^2 in pH=7.01 buffer) indicates that the thermodynamic quality of the solvent at 21 °C is close to ideal (θ solvent). M_w=30200±1500 Da in buffer, pH=7.01 is close to that expected from the degree of polymerization of PACh, *i.e.*, the polymer synthesis reaction is not complicated by side crosslinking reactions. Intrinsic viscosity [η] = 9.7 см^3/г$^{-1}$ measured in buffer pH=7.01, is in accordance with hydrodynamic radius.

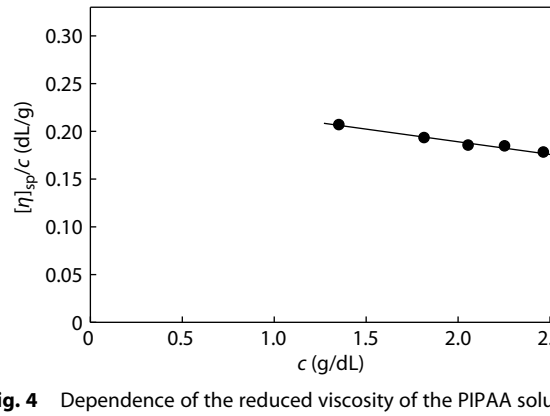

Fig. 4 Dependence of the reduced viscosity of the PIPAA solution in water at pH=6.8 on the polymer concentration.

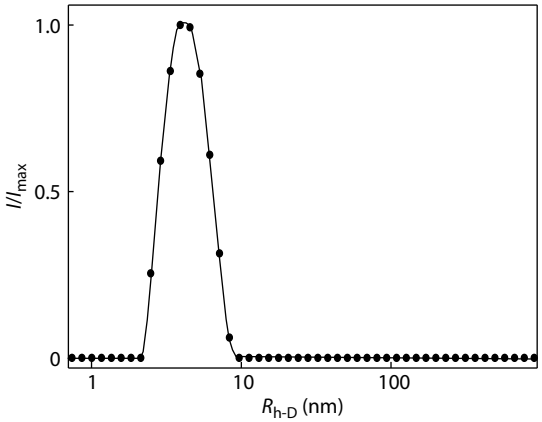

Fig. 5 Hydrodynamic radii distribution for solution of PIPAA at c=0.0110 g·cm^{-3} in buffer pH=7.01. I_{max} is maximum intensity of scattered light for given solution concentration.

Behavior of PIPAA in Buffer Solutions

We studied PIPAA in water and in buffer solutions (Table 1) commonly used in biology-related experiments: sodium-potassium phosphate (pH 6.86 and 7.01), sodium phosphate (pH 7.40), and HEPES-based buffers (pH 7.20 and 7.35). All solutions contain particles with a radius of about 3 nm at room temperature, which corresponds to individual PIPAA macromolecules. Aqueous PIPAA solution contains 86 nm aggregates, a slight increase in pH (6.76 to 7.10) results in PIPAA insolubility, and buffer solutions do not contain large particles, including pH 7.40.

Kinetics of PIPAA aggregation at elevated temperatures

The formation of interpolymer or polymer-metal complexes are relatively fast reactions. The equilibration time of these processes does not exceed several minutes in dilute solutions. The study of macromolecular reorganization under the influence of temperature change is usually carried out after a time corresponding to the thermal equilibration of the solution itself (several minutes). There are some evidences that thermo-sensitive polymers sometimes reach equilibrium after an hour or more.[51,52] Knowledge of the equilibrium time is important for the proper study of polymer solutions as well as for the design and application of complex structures based on thermo- and

https://doi.org/10.1007/s10118-023-3056-6

pH-sensitive polymers.

Transmission and scattering from PIPA solutions show no significant time dependence when heated below the phase separation beginning temperature (T_1). The system shows clear time dependences at T_1 (Fig. 6). The longest equilibrium time (t_{eq}) was observed at T_1 and the shortest at T_2 (temperature of the end of phase separation, Fig. 7). A typical dependence of particle size on time is shown in Fig. 7. The incubation period is 750 s, after which large particles become visible in the solution. This time cannot be explained by thermal equilibration of the cell, because the previous temperature was 0.5 °C lower with equilibration for 1000 s. The size of large particles decreases slightly after t_{eq}. Increasing the temperature after t_{eq} (Fig. 8) results in a similar time dependence of the particle size, and at 1.5 degrees above T_1 individual macromolecules are not visible after equilibration.

Temperature dependences of the characteristics of PIPAA in buffer solutions

We studied PIPAA solutions by heating in 1 °C increments, allowing them to stand for 1000 s, and measuring light transmittance and scattering at 90°. The equilibration time at temperature T_1 and higher was estimated as described above. Typical temperature dependences of light scattering intensity I and optical transmittance I^* are shown in Fig. 9 and Fig. 10, respectively. The values of T_1 and T_2 are the same with an accuracy of 0.5 °C when measured by I or I^*. In the case of sodium-potassium-phosphate buffer, T_1 and T_2 decreases with increasing pH and

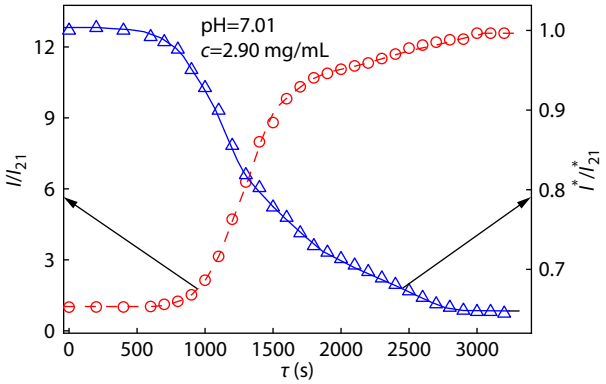

Fig. 6 Typical time dependences of relative optical transmission I^*/I^*_{21} and relative intensity of scattered light I/I_{21} for PIPAA in buffer solution at T_1 (29 °C).

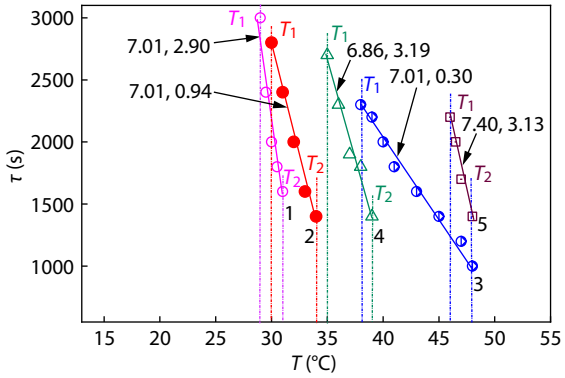

Fig. 7 Dependence of equilibration time on temperature. pH and concentration of PIPAA are shown near curves.

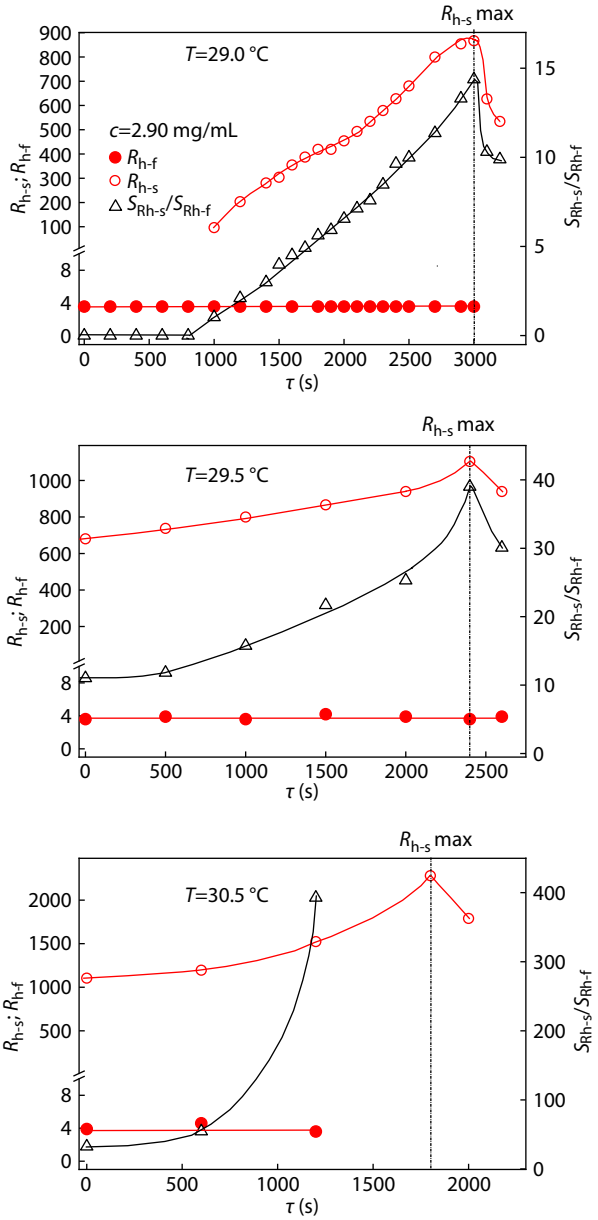

Fig. 8 Typical dependence of the particle radius ($R_{h\text{-}s}$ and $R_{h\text{-}f}$, nm) and the ratio of peak intensities ($S_{Rh\text{-}s}/S_{Rh\text{-}f}$) on the ageing time, pH=7.01. $R_{h\text{-}f}$—hydrodynamic radii of macromolecules; $R_{h\text{-}s}$—hydrodynamic radii of aggregates; $S_{Rh\text{-}f}$—area under the peak on the $I(R_{h\text{-}f})$ distribution curve corresponding to the fast mode; $S_{Rh\text{-}s}$—area under the peak in the $I(R_{h\text{-}s})$ distribution curve corresponding to the slow mode.

concentration. The interval $T_1 - T_2$ (ΔT) increases as the concentration decreases. Replacing potassium with sodium in the buffer causes a significant increase in T_1 and T_2 even at pH 7.40.

PIPAA buffer solutions contain small (about 3 nm) particles below T_1, and aggregates of several hundred nm appear at T_1 (Fig. 11). Individual macromolecules are undetectable at 0.5–1 °C above T_1, and aggregates increase in size up to T_2. Particle size decreases after T_2, but DLS measurements are not reliable in this area because of the high turbidity of the system.

https://doi.org/10.1007/s10118-023-3056-6

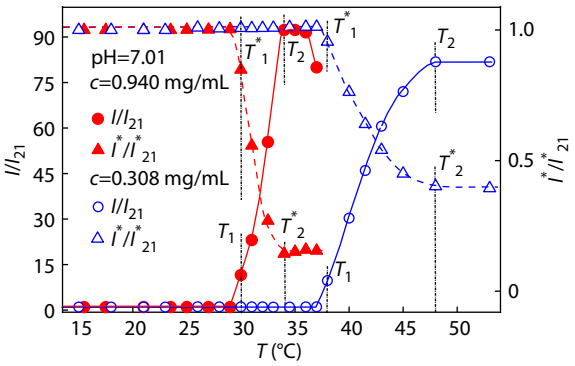

Fig. 9 Temperature dependences of the relative intensity of scattered light I/I_{21} and relative optical transmission I^*/I^*_{21} for PIPAA buffer solutions (pH=7.01). I_{21} and I^*_{21} are light scattering intensity and optical transmission at 21 °C.

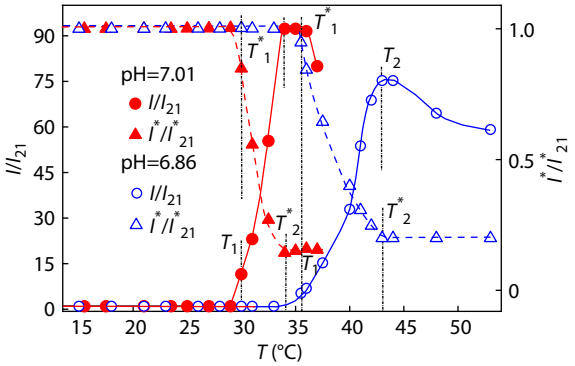

Fig. 10 Temperature dependences of the relative intensity of scattered light I/I_{21} and relative optical transmission I^*/I^*_{21} for PIPAA buffer solutions (pH=7.01, c=0.983 mg/mL and pH 6.86, c=0.940 mg/mL). I_{21} and I^*_{21} are light scattering intensity and optical transmission at 21 °C, respectively.

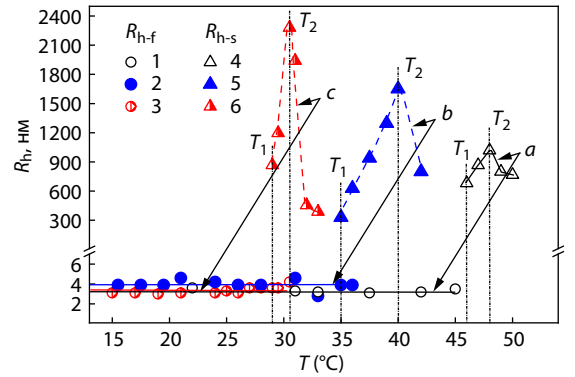

Fig. 11 The dependences of hydrodynamic radius R_h of scattering objects relative light scattering intensity I/I_{21} and optical transmission I^*/I^*_{21} on temperature for PIPAA buffer solutions. $R_{h\text{-}f}$—individual macromolecules, $R_{h\text{-}s}$—aggregates. (a) pH=7.01, c=2.902 mg/mL (1,4); (b) pH=6.86, c=2.994 mg/mL (2,5); (c) pH=7.40 (PBS), c=3.133 mg/mL (3,6).

Promising Applications of PIPAA

Oligonucleotide carriers

Polymeric amines are considered as carriers for DNA/RNA oligonucleotides in gene therapy.[53] With the first polymer in this area, polyethyleneimine (PEI), the effect of "proton sponge" was demonstrated.[54] Polymer-oligonucleotide complexes (polyplexes) are transported to cell organelles, endosomes, which contain an acidic environment and enzymes capable of degrading the oligonucleotide. Polymeric bases with high buffer capacity assimilate large amounts of acidic counterions, which leads to an increase in the ionic strength within the endosomes. This high ionic strength is compensated by additional water, causing the endosome to burst and the oligonucleotide to be released into the cytoplasm before being destroyed by enzymes. PIPAA at 20 and 40 °C shows a buffer capacity (Fig. 12) higher than PEI and PVI in the weakly acidic region, which makes PIPAA a promising structure for oligonucleotide carrier development. The ability of PIPAA to interact with oligonucleotides was confirmed by gel electrophoresis (Fig. 13). Stable polyplexes exist at an N:P ratio of 25:50, which is significantly lower than for PVI (500 for a sample of comparable molecular weight).[31] It has recently been shown[55] that the introduction of hydrophilic moieties into complex polymer structures can enhance their ability to bind nucleic acids even when the hydrophilic groups themselves are unable to interact with phosphate groups. Based on our results, we believe that imidazole-containing chains are promising for the design of complex gene delivery systems.

Functionalized coatings

Some biomedical applications need modified surfaces capable

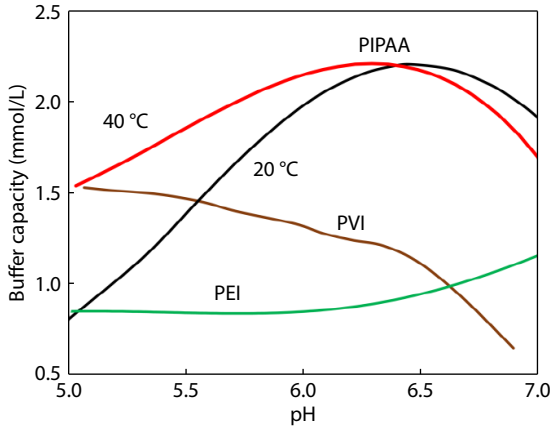

Fig. 12 Buffer capacity of PIPAA, PVI and polyethyleneimine (PEI) in 0.1 mol/L NaCl at 20 °C. PVI and PEI data are from our previous study.[31]

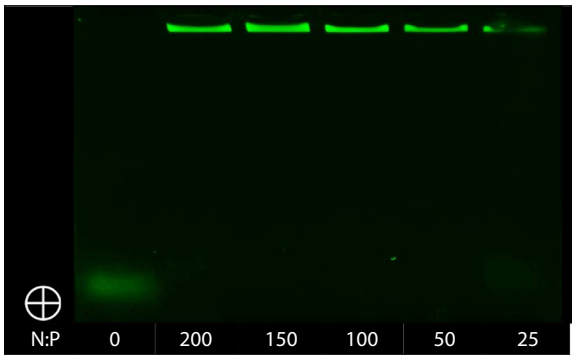

Fig. 13 Gel electrophoresis data for DNA oligonucleotide complex with new polymer. Lane 1—free oligonucleotide, N/P ratios are indicated in the first row.

of attaching various objects, such as living cells. These surfaces must carry some positive charge for better binding to negative cell membranes and be non-toxic. Amine groups are highly charged under physiological conditions, which causes their toxicity, so less basic imidazole units are more promising. The thermal sensitivity of PIPAA opens up additional possibilities for controlling surface properties. We prepared a 24-well microbiological plate coated with PIPAA cross-linked epichlorohydrin. The ability of the modified surface to attach negatively charged objects was tested with poly(acrylic acid) (PAA). PAA was visualized using the fluorescent amine NBD-N3.[42] The data presented in Fig. 14 show the stability of the coating after 7 days of storage in PBS buffer at 37 °C. The coatings exhibit micrometer-level surface roughness, which can improve cell attachment.

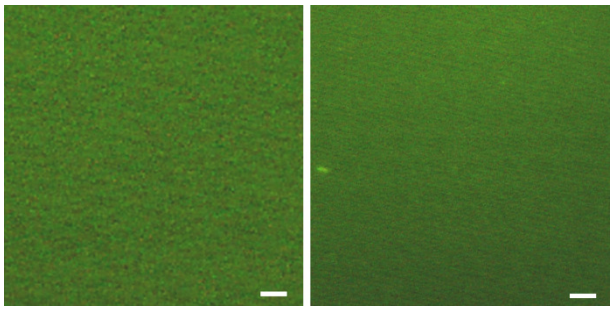

Fig. 14 Fluorescence images of cross-linked coatings of the bottom of a 24-well microbiological plate. Left: initial coating, right: after 7 days of storage in PBS buffer at 37 °C. The coatings were visualized under the action of PAA and the amine-containing dye NBD-N3. Scale bar represents 10 μm.

CONCLUSIONS

A new polymer containing an imidazole ring removed from the main chain by a five-bond spacer was obtained by modifying poly(acryloyl chloride). The basicity of the new polymer is less than that of the polymeric amines, which makes it pH-sensitive in the neutral pH range. The presence of methylene units in the side chain leads to the thermolability of the polymer at 29–48 °C and in the same neutral pH range. This behavior is quite different from polymers with side amine groups, whose thermolability is possible only at high pH values, where the amine groups are non-protonated. PIPAA has a higher basicity than polyvinylimidazole and a higher buffer capacity in the neutral region in the absence of toxic amino groups which is important for creating gene delivery systems and for cell immobilization. The ability of the new polymer to form complexes with oligonucleotides at physiological pH values was shown by gel electrophoresis.

In the future, it is possible to create PIPAA-based polymeric thermo- and pH-labile coatings with adjustable adhesive properties which are capable of attaching living cells without hindering their growth under certain conditions and of detaching them when conditions change to the physiological ones. Such materials and technologies are highly demanding for regenerative medicine, biotechnological production of proteins and other drugs, and creation of model cell cultures for fundamental and applied research.

Conflict of Interests

The authors declare no interest conflict.

ACKNOWLEDGMENTS

This work was financially supported by the Russian Science Foundation (No. 22-24-00474).

REFERENCES

1 Wei, M.; Gao, Y.; Li, X.; Serpe, M. J. Stimuli-responsive polymers and their applications. *Polym. Chem.* **2017**, *8*, 127–143.
2 Cabane, E.; Zhang, X.; Langowska, K.; Palivan, C. G.; Meier, W. Stimuli-responsive polymers and their applications in nanomedicine. *Biointerphases* **2012**, *7*, 9.
3 Bawa, P.; Pillay, V.; E Choonara, Y.; Toit, L. C. Stimuli-responsive polymers and their applications in drug delivery. *Biomed. Mater.* **2009**, *4*, 022001.
4 Gandhi, A.; Paul, A.; Sen, S. O.; Sen, K. K. Studies on thermoresponsive polymers: Phase behaviour, drug delivery and biomedical applications. *Asian J. Pharm. Sci.* **2015**, *10*, 99–107.
5 Kocak, G.; Tuncer, C.; Bütün, V. pH-Responsive polymers. *Polym. Chem*. **2017**, *8*, 144–176.
6 Ward, M. A.; Georgiou, T. K. Thermoresponsive polymers for biomedical applications. *Polymers* **2011**, *3*, 1215–1242.
7 Simonova, M. A.; Zakharova, N. V.; Khayrullin, A. R.; Filippov, A. P.; Annenkov, V. V. Behavior of double stimuli-responsive copolymer of *N*-(3-(diethylamino)propyl)-*N*-methylacrylamide and *N,N*-diethylacrylamide in aqueous solutions. Int. *J. Polym. Anal. Charact.* **2018**, *23*, 236–243.
8 Zakharova, N. V.; Simonova, M. A.; Filippov, A. P.; Zelinskiy, S. N.; Annenkov, V. V. Synthesis, molecular characteristics, and stimulus-sensitivity of graft-copolymer of chitosan poly(*N,N*-diethylacrylamide). *J. Molecular Liq.* **2019**, *292*, 111355.
9 Pilipenko, I. M.; Korzhikov-Vlakh, V. A.; Zakharova, N. V.; Tennikova, T. B.; Urtti, A. Thermo- and pH-sensitive glycosaminoglycans derivatives obtained by controlled grafting of poly(*N*-isopropylacrylamide). *Carbohydr. Polym.* **2020**, *248*, 116764.
10 Kyriakides, T.; Cheung, C.; Murthy, N., Bornstein, P.; Stayton, P.; Hoffman, A. J. pH-Sensitive polymers that enhance intracellular drug delivery *in vivo*. *Control. Rel*. **2002**, *78*, 295–303.
11 Drummond, D.; Zignani, M.; Leroux, J. Current status of pH-sensitive liposomes in drug delivery. *Prog. Lipid Res.* **2000**, *39*, 409–460.
12 Durfresne, M.; Garrec, D.; Sant, V.; Leroux, J.; Ranger, M. Preparation and characterization of water-soluble pH-sensitive nanocarriers for drug delivery. *Int. J. Pharmaceutics* **2004**, *277*, 81–90.
13 Gerasimov, O.; Boomer J.; Qualls M.; Thompson D. Cytosolic drug delivery using pH- and light-sensitive liposomes. *Adv. Drug Deliv. Rev.* **1999**, *38*, 317–338.
14 Liu, D.; Sun, J. Thermoresponsive Polypeptoids. *Polymers* **2020**, *12*, 2973.
15 Zhang, Y.; Broekhuis, A. A.; Stuart, M. C. A.; Picchioni, F. Polymeric amines by chemical modifications of alternating aliphatic polyketones. *J. Appl. Polym. Sci.* **2008**, *107*, 262–271.
16 Bütün, V.; Weaver, J. V. M.; Bories-Azeau, X.; Cai, Y.; Armes, S. P. A brief review of 'schizophrenic' block copolymers. *React. Funct. Polym.* **2006**, *66*, 157–165.
17 Smedt, S. C. D.; Demeester, J.; Hennink, W. E. Cationic polymer based gene delivery systems. *Pharm. Res.* **2000**, *17*, 113–126.
18 Allen, M. H. Jr.; Day, K. N.; Hemp, S. T.; Long, T. E. Synthesis of folic acid-containing imidazolium copolymers for potential gene delivery applications. *Macromol. Chem. Phys.* **2013**, *214*, 797–805.

19 Danilovtseva, E. N.; Krishnan, U. M.; Pal'shin, V. A.; Annenkov, V. V. Polymeric amines and ampholytes derived from poly(acryloyl chloride): synthesis, influence on silicic acid condensation and interaction with nucleic acid. *Polymers* **2017**, *9*, 624.
20 Ofridam, F.; Tarhini, M.; Lebaz, N.; Gagnière, É.; Mangin, D.; Elaissari, A. pH-sensitive polymers: classification and some fine potential applications. *Polym. Adv. Technol.* **2021**, *32*, 1455–1484.
21 Oda, Y.; Kanaoka, S.; Aoshima, S. Synthesis of dual pH/temperature-responsive polymers with amino groups by living cationic polymerization. *J. Polym. Sci., Part A: Polym. Chem.* **2010**, *4*, 1207–1213.
22 Gil, E. S.; Hudson, S. M. Stimuli-responsive polymers and their bioconjugate. *Prog. Polym. Sci.* **2004**, *29*, 1173–1222.
23 SPARC. pKa/property server. Ver 4.2 Mar. 2008. Available from, as of October 28, 2009: https://ibmlc2.chem.uga.edu/sparc/ .
24 Albert, A. *Heterocyclic chemistry*. 2nd Ed.; Athlone Press, **1968**.
25 Sundberg, R. J.; Martin, R. B. Interactions of histidine and other imidazole derivatives with transition metal ions in chemical and biological systems. *Chem. Rev.* **1974**, *74*, 471–517.
26 Nozaki, Y.; Gurd, F. R. N.; Chen, R. F.; Edsall, J. T. The association of 4-methylimidazole with the ions of cupric copper and zinc; with some observations on 2,4-dimethylimidazole. *J. Am. Chem. Soc.* **1957**, *79*, 2123–2129.
27 Pozdnyakov, A. S.; Emel'yanov, A. I.; Korzhova, S. A.; Kuznetsova, N. P.; Bolgova, Y. I.; Trofimova, O. M.; Semenova, T. A.; Prozorova, G. F. Green synthesis of stable nanocomposites containing copper nanoparticles incorporated in poly-*N*-vinylimidazole. *Polymers* **2021**, *13*, 3212.
28 Luo, X. F.; Goh, S. H.; Lee, S. Y. Miscibility and interpolymer complexation of poly(1-vinylimidazole) with hydroxyl- and carboxyl-containing polymers. *Makromol. Chem. Phys.* **1999**, *200*, 399–404.
29 Isikli, S.; Tuncagil, S.; Bozkurt, A.; Toppare, L. Immobilization of invertase in a novel proton conducting poly(vinylphosphonic acid—poly(1-vinylimidazole) network. *J. Macromol. Sci. Part A* **2010**, *47*, 639–646.
30 Asayama, S.; Nishinohara, S.; Kawakami, H. Zinc-chelated poly(1-vinylimidazole) and a carbohydrate ligand polycation form DNA ternary complexes for gene delivery. *Bioconjugate Chem.* **2011**, *22*, 1864–1868.
31 Danilovtseva, E. N.; Zelinskiy, S. N.; Pal'shin, V. A.; Kandasamy, G.; Krishnan, U. M.; Annenkov, V. V. Poly(1-vinylimidazole) prospects in gene delivery. *Chinese J. Polym. Sci.* **2019**, *37*, 637–645.
32 Mazyar, N. L.; Annenkov, V. V.; Kruglova, V. A.; Ananiev, S. M.; Danilovtseva, E. N.; Rokhin, A. V.; Zinchenko, S. V. Acid-base properties of poly(1-vinylazoles) in aqueous solution. *Rus. Chem. Bull. Intern. Ed.* **2000**, *49*, 2013–2017.
33 Sharma, A.; Srivastava, A. Pronounced influence of pH, metal-ion and solvent isotope on the thermoresponse of synthetic amphiphilic polypeptides. *Polym. Chem*. **2013**, *4*, 5119–5128.
34 Seo, K.; Kim, D. Phase transition behavior of novel pH-sensitive polyaspartamide derivatives grafted with 1-(3-aminopropyl)imidazole. *Macromol. Biosci.* **2006**, *6*, 758–766.
35 Bogomolova, A.; Kaberov, L.; Sedlacek, O.; Filippov, S. K.; Stepanek, P.; Král, V.; Wang, X. Y.; Liu, S. L.; Ye, X. D.; Hruby, M. Double stimuli-responsive polymer systems: how to use crosstalk between pH- and thermosensitivity for drug depots. *Eur. Polym. J.* **2016**, *84*, 54–64.
36 Naka, K.; Masuoka, S.; Shinke, R.; Yamada, M. Synthesis of first- and second-generation imidazoleterminated POSS-core dendrimers and their pH responsive and coordination properties. *Polym. J.* **2012**, *44*, 353–359.
37 Handel, T. M.; Ponticello, I. S.; Tan, J. S. Effects of side-chain structure on polymer conformation: synthesis and dilute solution properties. *Macromolecules* **1987**, *20*, 264–267.
38 Zakharova, N. V.; Filippov, A. P.; Zelinskii, S. N.; Danilovtseva, E. N.; Annenkov, V. V. The influence of composition of thermo- and pH-sensitive copolymers of *N*-(3-(diethylamino)propyl)-*N*-methylacrylamide and *N,N*-diethylacrylamide on their behavior in aqueous solutions. *Polym. Sci. A* **2019**, *61*, 1–8.
39 Annenkov, V. V.; Danilovtseva, E. N.; Zelinskiy, S. N.; Basharina, T. N.; Safonova, T. A.; Korneva, E. S.; Likhoshway, Ye. V.; Grachev, M. A. Novel fluorescent dyes based on oligopropylamines for the *in vivo* staining of eukaryotic unicellular algae. *Anal. Biochem.* **2010**, *407*, 44–51.
40 Annenkov, V. V.; Danilovtseva, E. N.; Likhoshway, Y. V.; Patwardhan, S. V.; Perry C. C. Controlled stabilisation of silicic acid below pH 9 using poly(1-vinylimidazole). *J. Mater. Chem.* **2008**, *18*, 553–559.
41 Buruiana, E.C.; Buruiana, T.; Hahui, L. Preparation and characterization of new optically active poly(*N*-acryloyl chloride) functionalized with (*S*)-phenylalanine and pendant pyrene. *J. Photochem. Photobiol. A* **2007**, *189*, 65–72.
42 Sandeli, E. B.; West, T. S. Recommended nomenclature for titrimetric analysis. *Pure Appl. Chem.* **1969**, *18*, 427–436.
43 Danilovtseva, E. N.; Verkhozina, O. N.; Zelinskiy, S. N.; Ivanov, N. A.; Tsiganov, P.Y.; Basharina, T. N.; Annenkov, V. V. New fluorescent derivatives of oligopropylamines. *ARKIVOC* **2013**, *3*, 266–281.
44 González-de-Castro, Á.; Broughton, H.; Martínez-Pérez, J. A.; Espinosa, J. F. Conformational features of secondary *N*-cyclopropyl amides. *J. Org. Chem.* **2015**, *80*, 3914–3920.
45 Lanyon-Hogg, T.; Ritzefeld, M.; Masumoto, N.; Magee, A. I.; Rzepa, H. S.; Tate, E. W. Modulation of amide bond rotamers in 5-acyl-6,7-dihydrothieno[3,2-*c*]pyridines. *J. Org. Chem.* **2015**, *80*, 4370–4377.
46 Lippert, J. L.; Robertson, J. A.; Havens, J. R.; Tan, J. S. Structural studies of poly(*N*-vinylimidazole) complexes by infrared and Raman spectroscopy. *Macromolecules* **1985**, *18*, 63–67.
47 Katchalsky, A.; Mazur, J.; Spitnik, P. SECTION II: General behavior of biocolloids and polyelectrolytes in solution (continued) polybase properties of polyvinylamine. *J. Polym. Sci.* **1957**, *23*, 513–532.
48 Nekrasova, T. N.; Gabrielyan, A. G.; Ptitsyn, O. B. Determination of the thermodynamic characteristics of the conformational transition in polymethacrylic acid from potentiometric titration curves. *Polym. Sci. U.S.S.R.* **1968**, *10*, 348–355.
49 Kratochvil, P. in *Classical light scattering from polymer solutions*. Elsevier: Amsterdam, The Netherlands, **1987**, 334.
50 Schartl, W. in *Light scattering from polymer solutions and nanoparticle dispersions*. Springer: Berlin, Germany, **2007**, 175.
51 Amirova, A. I.; Dudkina, M. M.; Tenkovtsev, A. V.; Filippov, A. P. Self-assembly of star-shaped poly(2-isopropyl-2-oxazoline) in aqueous solutions. *Colloid. Polym. Sci.* **2015**, *293*, 239–248.
52 Filippov, A. P.; Tarabukina, E. B.; Zakharova, N. V.; Amirova, A. I.; Simonova, M. A. Behaviorial features of aqueous solutions of thermoresponsive and pH-sensitive polymers with complicated architectures. *Fiber Chem.* **2015**, *47*, 137–143.
53 Annenkov, V. V.; Krishnan, U. M.; Pal'shin, V. A.; Zelinskiy, S. N.; Kandasamy, G.; Danilovtseva, E. N. Design of oligonucleotide carriers: importance of polyamine chain length. *Polymers* **2018**, *10*, 1297.
54 Boussif, O.; Lezoualc'h, F.; Zanta, M. A.; Mergny, M. D.; Scherman, D. A.; Demeneix, B.; Behr, J. P. A versatile vector for gene and oligonucleotide transfer into cells in culture and *in vivo*: polyethylenimine. *Proc. Natl. Acad. Sci. U. S. A.* **1995**, *92*, 7297–7301.
55 Hu, X.; Li, Y.; Liu, T.; Zhang, G.; Liu, S. Photodegradable neutral-cationic brush block copolymers for nonviral gene delivery. *Chem. Asian J.* **2014**, *9*, 2148–2155.

https://doi.org/10.1007/s10118-023-3056-6